

EUROPEAN COOPERATION
IN THE FIELD OF SCIENTIFIC
AND TECHNICAL RESEARCH

COST 2100 TD(08) 407
Wroclav, Poland
February 6-8, 2008

EURO-COST

SOURCE: Institute Eurecom

Real-time Multi-user MIMO Channel Sounding and Capacity Evaluations

Florian Kaltenberger, Leonardo Cardoso, Marios Kountouris,
Raymond Knopp, David Gesbert
2229, Route des Cretes - B.P. 193
06904 Sophia Antipolis, France
Phone: +33 4 93 00 81 86
Fax: +33 4 93 00 82 00
Email: florian.kaltenberger@eurecom.fr

Abstract

In multi-user multiple-input multiple-output (MU-MIMO) systems, spatial multiplexing can be employed to increase the throughput without the need for multiple antennas and expensive signal processing at the user equipments. In theory, MU-MIMO is also more immune to most of propagation limitations plaguing single-user MIMO (SU-MIMO) systems, such as channel rank loss or antenna correlation. In this paper we compare the sum rate capacity of different MU-MIMO precoding schemes such as dirty paper coding (DPC) and linear precoding to SU-MIMO using real channel measurement data. The measurement data has been acquired using Eurecom's MIMO Openair Sounder (EMOS). The EMOS can perform real-time MIMO channel measurements synchronously over multiple users. The results show that the sum rate capacity in the measured channels is worse than the one in the uncorrelated synthetic channel. However, even in the measured channels DPC increases the sum rate capacity by a factor of 3.2 compared to SU-MIMO at high SNR using four transmit and four users with one receive antenna each. Linear precoding still increases the sum rate capacity by a factor of 2.7 at high SNR but provides little gains at low SNR.

1 Introduction

A multi-user multiple-input multiple-output (MU-MIMO) system refers to a scenario where a base-station (BS) employing multiple antennas communicates with several users simultaneously. The users can have multiple antennas too, but this is not a necessity. The uplink channel is also referred to as multiple access channel (MAC), whereas the downlink channel is called a broadcast channel (BC) [1].

In this paper we confine ourselves to the broadcast channel. Information theory reveals that if the channel is fully known at the transmitter, the optimum transmit strategy for the MU-MIMO broadcast channel involves a theoretical pre-interference cancelation technique known as dirty paper coding (DPC) combined with an implicit user scheduling and power loading algorithm [2]. However, DPC is very computationally expensive and thus simpler, linear transmit strategies such as zero forcing (ZF) and minimum mean square error (MMSE) precoding have been proposed [3].

Compared to a single-user MIMO (SU-MIMO) time division multiple access (TDMA) system, MU-MIMO can bring a theoretical performance gain of up to $\max(\min(M/N, K), 1)$ in an independent and identically distributed (i.i.d.) Rayleigh fading channel, where M and N is the number of transmit antennas and receive antennas respectively and K is the number of users [4]. However, little is known about the performance of MU-MIMO schemes in real-world channels.

In this paper we compare the performance of MU-MIMO using DPC and MMSE precoding to SU-MIMO TDMA based on real channel measurements. We do not study the impact of user scheduling or power control. Realistic MU-MIMO channel measurements have been obtained using Eurecom's MIMO Openair Sounder (EMOS) [5]. The EMOS can perform real-time channel measurements synchronously over multiple users moving at vehicular speed. For this paper, we have used four transmit antennas and four users with two antennas each. The measured channels are used to calculate the capacity offline, assuming a perfect feedback channel.

To the best of our knowledge, no such comparison based on real MU channel measurements has been reported. Real indoor channel measurements have been used in [6, 7] for the evaluation of the proposed MU-MIMO scheme. Real outdoor channel measurements have been used in [8] to study limited feedback. However, the channel measurements were obtained with one receiver at different times and not synchronously as in our measurements.

Various comparisons based on synthetic MIMO channels with i.i.d. elements have been reported in [4, 9, 10, 11]. The main contribution of these works was to derive bounds on the gain of DPC over SU-MIMO TDMA as well as linear MU-MIMO precoding methods for high SNR, or a large number

of antennas and users. The performance of BD in correlated MIMO channels has been studied in [12] and [3] provides simulation results for MU-MIMO with regularized channel inversion.

The paper is organized as follows. We introduce the signal model and the different MU-MIMO precoding schemes in Sections 2 and 3.2 respectively. In Section 4 we describe the EMOS in some more detail and explain how the channel measurements are performed. In Section 5 the measurement campaign is described and results are discussed. We finally give conclusions in Section 6.

2 System Model

We consider a multi-user, multi-antenna downlink channel in which a base station (BS) equipped with M antennas communicates with $K \leq M$ terminals, each equipped with N antennas. The received signal $\mathbf{y}_{k,m,q} \in \mathbb{C}^{N \times 1}$ of the k -th user at time m and frequency q is mathematically described as

$$\mathbf{y}_{k,m,q} = \mathbf{H}_{k,m,q} \mathbf{x}_{m,q} + \mathbf{n}_{k,m,q} \quad \text{for } k = 1, \dots, K \quad (1)$$

where $\mathbf{H}_{k,m,q} \in \mathbb{C}^{N \times M}$ represents the k -th user channel response at time m and frequency q , $\mathbf{x}_{m,q} \in \mathbb{C}^{M \times 1}$ is the vector of transmitted symbols at time m and frequency q , and $\mathbf{n}_{k,m,q} \in \mathbb{C}^{N \times 1}$ is i.i.d. circularly symmetric additive complex Gaussian noise with zero mean and variance σ^2 , $\forall k$. We assume that each of the receivers has perfect and instantaneous knowledge of its own channel. The transmitter is subject to an average power constraint, i.e. $\mathbb{E}\{\mathbf{x}_{m,q}^H \mathbf{x}_{m,q}\} \leq P$, which implies that the total transmit power is not dependent on the number of transmit antennas. For notation convenience, in the following sections we drop the time and frequency indices.

3 Sum Rate Capacity

In this section we review the sum rate capacity of a MU-MIMO system assuming DPC and linear precoding as well as the capacity of SU-MIMO TDMA system.

3.1 Dirty Paper Coding

From the results in [2, 13, 14, 15], the sum capacity of the BC can be expressed by the following maximization:

$$\mathcal{C}_{\text{BC}}(\mathbf{H}_1, \dots, \mathbf{H}_K, P) = \max_{\mathbf{\Sigma}_k \geq 0, \sum_{k=1}^K \text{tr}(\mathbf{\Sigma}_k) \leq P} \sum_{k=1}^K \log_2 \frac{\left| \mathbf{I} + \mathbf{H}_k \left(\sum_{j=1}^K \mathbf{\Sigma}_j \right) \mathbf{H}_k^H \right|}{\left| \mathbf{I} + \mathbf{H}_k \left(\sum_{j \neq k} \mathbf{\Sigma}_j \right) \mathbf{H}_k^H \right|}, \quad (2)$$

where the maximization is over the set of all positive semidefinite transmit covariance matrices $\mathbf{\Sigma}_k, k = 1, \dots, K$. The above formula assumes that user codes drawn from an i.i.d. Gaussian distribution are used. However, the formula can also be used as an approximation for finite constellations assuming a constellation order higher than the channel capacity and an appropriate coding scheme.

The objective function of the maximization in (2) is a concave function of the covariance matrices, making it very difficult to deal with. Fortunately, due to the MAC-BC duality, the sum rate capacity of the MIMO BC is equal to the sum rate capacity of the dual MAC with power constraint P

$$\mathcal{C}_{\text{BC}}(\mathbf{H}_1, \dots, \mathbf{H}_K, P) = \mathcal{C}_{\text{MAC}}(\mathbf{H}_1, \dots, \mathbf{H}_K, P) = \max_{\mathbf{Q}_k \geq 0, \sum_{k=1}^K \text{tr}(\mathbf{Q}_k) \leq P} \log_2 \left| \mathbf{I} + \sum_{k=1}^K \mathbf{H}_k \mathbf{Q}_k \mathbf{H}_k^H \right|, \quad (3)$$

where each of the matrices \mathbf{Q}_i is a positive semidefinite covariance matrix. Since (3) involves the maximization of a concave function, efficient numerical algorithms exist. In this paper, we use the specialized algorithm developed in [16] to calculate $\mathcal{C}_{\text{BC}}(\mathbf{H}_1, \dots, \mathbf{H}_K, P)$.

It has been shown that the sum rate capacity given in Equation (3) is actually achievable by a technique called dirty paper coding (DPC), i. e., $\mathcal{R}_{\text{DPC}}(\mathbf{H}_1, \dots, \mathbf{H}_K, P) = \mathcal{C}_{\text{BC}}(\mathbf{H}_1, \dots, \mathbf{H}_K, P)$. DPC pre-subtracts interference at the transmitter. However, DPC is very complex and difficult to implement. Thus we also study the linear precoding schemes in the next section.

3.2 Linear Precoding

Let $\mathbf{s}_k \in \mathbb{C}^{N \times 1}$ denote the k -th user transmit symbol vector. Under linear precoding, the transmitter multiplies the data symbol for each user k by a precoding matrix $\mathbf{W}_k \in \mathbb{C}^{M \times N}$ so that the transmitted signal is a linear function $\mathbf{x} = \sum_{k=1}^K \mathbf{W}_k \mathbf{s}_k$. The resulting received signal vector for user k is given by

$$\mathbf{y}_k = \mathbf{H}_k \mathbf{W}_k \mathbf{s}_k + \sum_{j \neq k} \mathbf{H}_k \mathbf{W}_j \mathbf{s}_j + \mathbf{n}_k \quad (4)$$

where the second-term in (4) represents the multi-user interference. We assume that each user will decode $S \leq N$ streams that constitute its data. The goal of linear precoding is to design $\{\mathbf{W}_k\}_{k=1}^K$ based on the channel matrix knowledge, so a given performance metric is maximized for each stream.

3.2.1 Zero-Forcing Precoding (Channel Inversion)

For ease of exposition, we assume $N = 1$ and we define $\mathbf{H} = [\mathbf{h}_1^T \dots \mathbf{h}_K^T]^T$. The unit-norm beamforming vector of user k is denoted as $\mathbf{w}_k \in \mathbb{C}^{M \times 1}$, $k = 1, \dots, K$.

A standard suboptimal approach providing a promising tradeoff between complexity and performance is zero-forcing precoding, also known as channel inversion. In ZF, the precoder is designed to achieve zero interference between the users, i.e., $\mathbf{h}_k \mathbf{w}_j = 0$ for $j \neq k$. The ZF precoding matrix is given by the Moore-Penrose pseudoinverse of \mathbf{H}

$$\mathbf{W} = \mathbf{H}^\dagger = \mathbf{H}^H (\mathbf{H} \mathbf{H}^H)^{-1} \quad (5)$$

where \mathbf{w}_k is obtained by normalizing the k -th column of \mathbf{W} .

Assuming equal power allocation over the users, the achievable sum rate is given by

$$\mathcal{R}_{\text{ZF}} = \sum_{k=1}^K \log_2 \left(1 + \frac{P}{K \sigma^2} |\mathbf{h}_k \mathbf{w}_k|^2 \right) \quad (6)$$

When the channel is ill-conditioned, at least one of the singular values of $(\mathbf{H} \mathbf{H}^H)^{-1}$ is very large, resulting in a very low SNR at the receivers. Note also that ZF precoding—in contrast to ZF (least-squares) equalization at the receive side which causes noise enhancement when the channel is nearly rank deficient—incurrs an excess transmission power penalty. Therefore, the capacity of channel inversion with no user selection does not increase linearly with M , unlike the optimum capacity.

3.2.2 MMSE Precoding (Regularized Channel Inversion)

For rank-deficient channels, the performance of ZF precoding can be improved by a regularization of the pseudo-inverse, which can be expressed as:

$$\mathbf{W} = \mathbf{H}^H (\mathbf{H} \mathbf{H}^H + \beta \mathbf{I})^{-1} \quad (7)$$

where β is a regularization factor. The above scheme is often referred to as Minimum Mean Square-Error (MMSE) precoding due to the analogous with MMSE beamforming weight design criterion if the noise is spatially white. The achievable throughput is given by

$$\mathcal{R}_{\text{MMSE}} = \sum_{k=1}^K \log_2(1 + \text{SINR}_k) \quad (8)$$

where SINR_k is described by

$$\text{SINR}_k = \frac{|\mathbf{h}_k \mathbf{w}_k|^2}{\sum_{j \neq k} |\mathbf{h}_k \mathbf{w}_j|^2 + K\sigma^2/P} \quad (9)$$

and \mathbf{w}_k is the normalized k -th column of the precoder given in (7).

Similarly to MMSE equalization, a non-zero β value results in a measured amount of multi-user interference. The amount of interference is determined by $\beta > 0$ and an optimal tradeoff between the condition of the channel matrix inverse and the amount of crosstalk ought to be found. In practice, the regularization factor is commonly chosen as $\beta = M\sigma^2/P$ motivated by the results in [3] that show that it approximately maximizes the SINR at each receiver, and leads to linear capacity growth with M . The performance of MMSE is certainly significantly better at low SNR and converges to that of ZF precoding at high SNR. However, MMSE does not provide parallel and orthogonal channels and thus power allocation techniques cannot be performed in a straightforward manner.

3.3 Time Division Multiple Access

The capacity of a single user k is given by

$$\mathcal{C}(\mathbf{H}_k, P) = \max_{\mathbf{Q}_k \geq 0, \text{tr}(\mathbf{Q}_k) \leq P} \log_2 |\mathbf{I} + \mathbf{H}_k \mathbf{Q}_k \mathbf{H}_k^H|. \quad (10)$$

The maximum is achieved by choosing the covariance matrix \mathbf{Q}_k to be along the eigenvectors of the matrix $\mathbf{H}_k \mathbf{H}_k^H$ and by choosing the eigenvalues according to the water filling procedure [17].

The maximum sum rate capacity is achieved by transmitting to the user with the largest single-user capacity. However, in this paper we assume that all users are served fairly proportional in a round robin fashion, i. e., we treat each \mathbf{H}_k as a different realization.

4 The EMOS Multi-user Platform

4.1 Hardware Description

The Eurecom MIMO Openair Sounder (EMOS) is based on the OpenAir hardware/software development platform at Eurecom. The platform consists of a BS that continuously sends a signaling frame, and one or more user equipments (UEs) that receive the frames to estimate the channel. For the BS, an ordinary server PC with four PLATON data acquisition cards (see Fig. 1(a)) is employed along with a Powerwave 3G broadband antenna (part no. 7760.00) composed of four elements which are arranged in two cross-polarized pairs (see Fig. 1(b)).

The UEs consist of an ordinary laptop computer with Eurecom's dual-RF CardBus/PCMCIA data acquisition card (see Fig. 1(c)) and two clip-on 3G Panorama Antennas (part no. TCLIP-DE3G, see Fig. 1(d)). The platform is designed for a full software-radio implementation, in the sense that all protocol layers run on the host PCs under the control of a Linux real time operation system.

Parameter	Value
Center Frequency	1917.6 kHz
Bandwidth	4.8MHz
BS Transmit Power	30 dBm
Number of Antennas at BS	4 (2 cross polarized)
Number of UE	4
Number of Antennas at UE	2
Number of Subcarriers	160

Table 1: EMOS Parameters

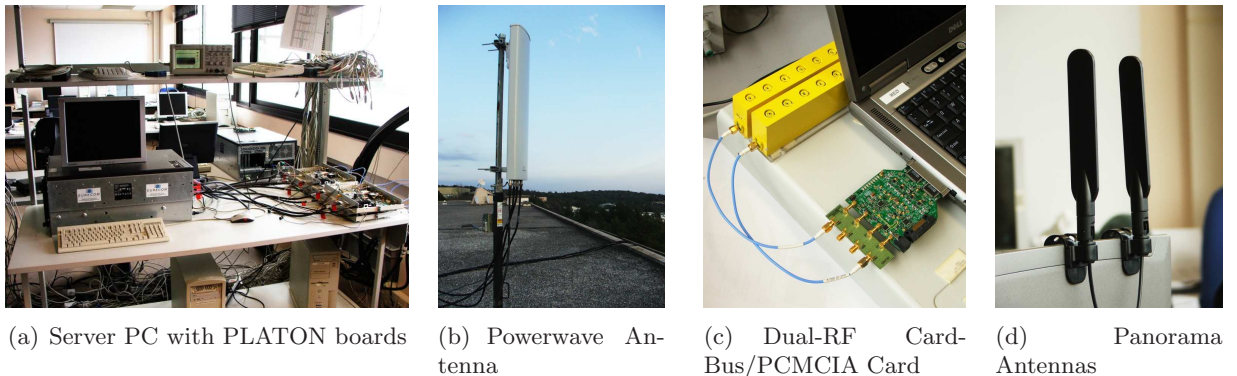


Figure 1: EMOS base-station and user equipment [5]

4.2 Sounding Signal

The EMOS is using an OFDM modulated sounding sequence. One transmit frame is 2.667 ms long and consists of a synchronization symbol (SCH), a broadcast data channel (BCH) comprising 7 OFDM symbols, a guard interval, and 48 pilot symbols used for channel estimation (see Fig. 2). The pilot symbols are taken from a pseudo-random QPSK sequence defined in the frequency domain. The subcarriers of the pilot symbols are multiplexed over the four transmit antennas to ensure orthogonality in the spatial domain. The BCH contains the frame number of the transmitted frame that is used for synchronization among the UEs. The details of the modulation and coding scheme for the BCH can be found on the OpenAirInterface website¹.

4.3 Channel Estimation Procedure

Each UE first synchronizes to the BS using the SCH. It then tries to decode the data in the BCH. If the BCH can be decoded successfully, then the channel estimation procedure is started.

The channel estimation procedure consists of two steps. First, the phase-shift noise generated by the dual-RF CardBus/PCMCIA card is suppressed using a phase derotation. Generated by the RF circuit, the phase-shift noise was observed to have a slow variation characteristic. We therefore model the phase-shift noise as being constant for each OFDM symbol and different for different OFDM symbols. We calculate the phase shift of every pilot symbol with respect to the first pilot symbol, which is used as a reference.

Secondly, the MIMO channel is estimated. To reduce the effects of white noise, we use the

¹<http://www.openairinterface.org>

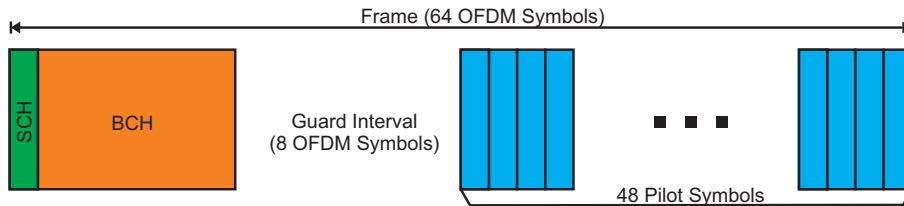


Figure 2: Frame structure of the OFDM Sounding Sequence.

average of all the derotated pilot symbols to estimate the channel. The estimated channel is then stored to disk. For a more detailed description of the channel estimation procedure see [5].

4.4 Multi-user Measurement Procedure

In order to conduct multi-user measurements, all the UEs need to be frame-synchronized by the BS. This is achieved by storing the frame number encoded in the BCH along with the measured channel at the UEs. This way, the measured channels can be aligned for later evaluations. The frame number is also used to synchronize the data acquisition between UEs. One measurement run (file) starts every 22.500 frames (60sec) and is exactly 18.750 frames (50sec) long.

5 Measurements and Results

5.1 Measurement Description

The measurements were conducted outdoors in the vicinity of the Eurecom institute. The scenario is characterized by a semi-urban hilly terrain, composed by short buildings and vegetation. Fig. 3 shows a map of the environment. The BS is located at the roof of one of the Eurecom buildings. The antenna is directed towards Garbejaire, a small nearby village.

The UEs were placed inside standard passenger cars. The cars were only allowed to go to places with an RSSI > -90 dBm, so that they can still decode the BCH. This means that the UEs were in line of sight (LOS) of the BS most of the time. Otherwise, the cars had no fixed routes.

For the presentation in this paper we selected one single measurement run of 50 sec duration. To ensure a constant average noise variance at the UEs, the channel of every user is normalized over the whole measurement run.

5.2 Results and Discussion

We compare the performance of MU-MIMO with linear MMSE precoding and DPC with that of a SU-MIMO TDMA scheme based on the empirical cumulative density function (CDF) of the sum rate capacity as well as the ergodic sum rate capacity (see Equations (3), (8), and (10)). We do not plot results for ZF precoding, since its performance is inferior to MMSE precoding at low SNR and equivalent to MMSE at high SNR [18].

In Fig. 4 we compare the CDF of the sum rate of SU-MIMO TDMA to MU-MIMO using a linear MMSE precoder and DPC respectively. There are four UEs with one receive antenna each (we ignore the second antenna). We show results for i.i.d. frequency-flat Rayleigh fading channel as well as the measured channel. The average SNR is fixed to 10dB for each user.

In Fig. 5 we compare the CDF of the sum rate of SU-MIMO TDMA, MU-MIMO MMSE and MU-MIMO DPC using four UEs with two receive antennas each. For the MMSE precoder we use

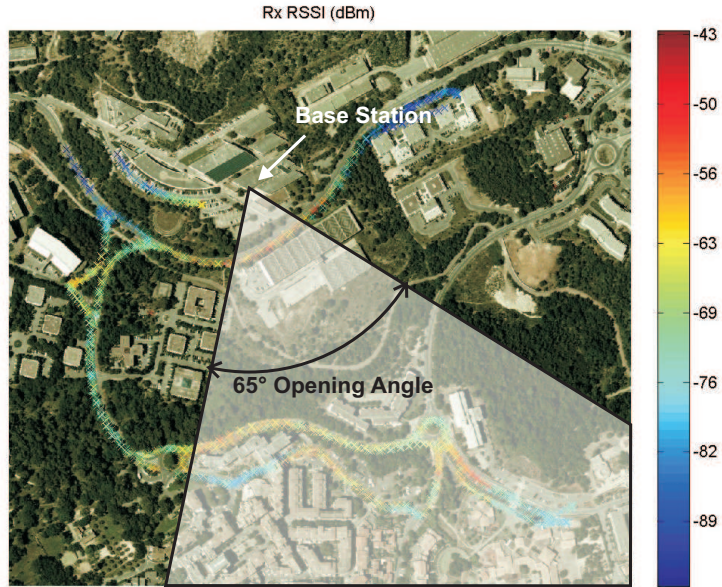


Figure 3: Map showing the RSSI along the measurement routes. The position and the opening angle of the BS antenna are also indicated.

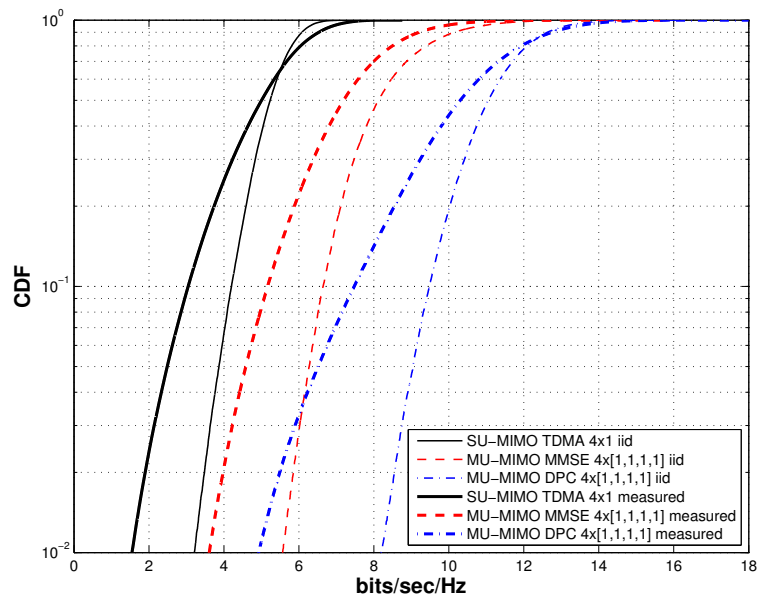


Figure 4: CDF of the sum rate capacity of SU-MIMO TDMA compared to MU-MIMO using a linear MMSE precoder and dirty paper precoding for one receive antenna. Results are shown for i.i.d. Rayleigh fading channel (denoted “i.i.d.”) as well as for the measured channel (denoted “meas.”). The average SNR is fixed to 10dB for each user.

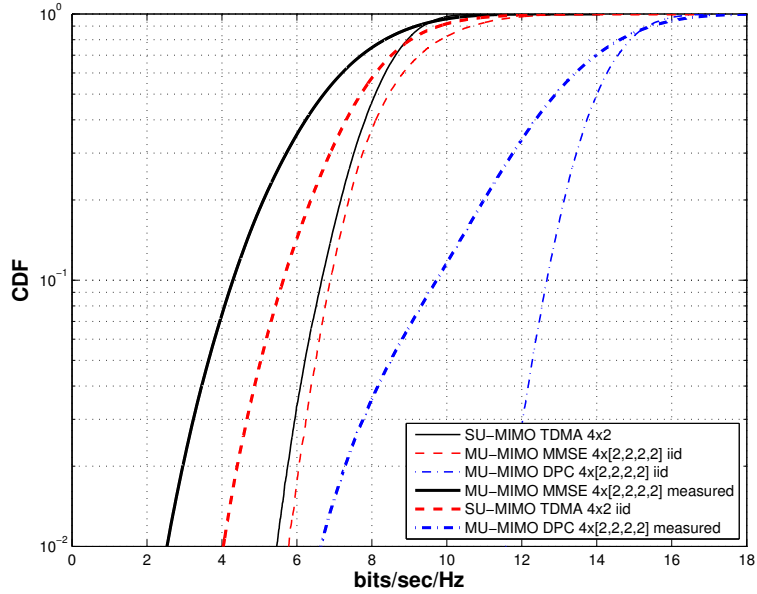


Figure 5: CDF of the sum rate capacity of SU-MIMO TDMA compared to MU-MIMO using a linear MMSE precoder with AS and dirty paper precoding for two receive antennas. Results are shown for i.i.d. Rayleigh fading channel (denoted “i.i.d.”) as well as for the measured channel (denoted “meas.”). The average SNR is fixed to 10dB for each user.

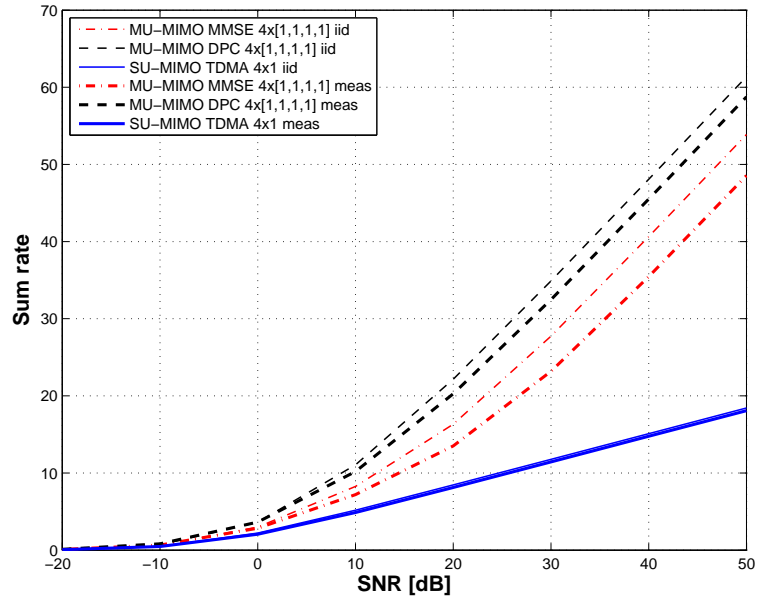


Figure 6: Ergodic (mean) sum rate capacity of SU-MIMO TDMA and MU-MIMO MMSSE and MU-MIMO DPC with one receive antenna. Results are shown for i.i.d. Rayleigh fading channel (denoted “i.i.d.”) as well as for the measured channel (denoted “meas.”).

the second receive antenna to perform antenna selection (AS): The wideband channel is grouped in chunks of 20 adjacent subcarriers and for every such chunk, the receive antenna with the higher energy (squared ℓ_2 norm) is selected.

Last but not least, we show in Figure 6 the ergodic (mean) sum rate capacity SU-MIMO TDMA, MU-MIMO MMMSE and MU-MIMO DPC with one receive antenna for up to an SNR of 50 dB.

It can be seen the performance of all the schemes is worse in the measured channel compared to the i.i.d. channels. In terms of ergodic sum rate capacity at high SNR (50 dB) SU-MIMO TDMA loses 0.3 bits/sec/Hz, MU-MIMO MMSE loses 5.3 bits/sec/Hz, and MU-MIMO DPC loses 2.6 bits/sec/Hz.

It can further be seen that MU-MIMO provides significant performance improvement over SU-MIMO. For example at 50 dB SNR MU-MIMO MMSE improves the performance by a factor of 2.7 and MU-MIMO DPC improves the performance by a factor of 3.2 in the measured channel.

6 Conclusions

We have presented capacity analysis of MU-MIMO precoding schemes using real channel measurement data. The data was acquired using Eurecom's MU-MIMO channel sounder EMOS.

The results confirm the theoretical results in the sense that MU-MIMO provides a higher sum rate capacity than SU-MIMO TDMA. Among the studied MU-MIMO schemes, DPC performs better than linear MMSE precoding at a higher computational cost. It is worth noting, that MU-MIMO with MMSE precoding and one receive antenna at each user even has a higher sum rate capacity than SU-MIMO TDMA with two receive antennas. Thus, the receiver design in MU-MIMO is greatly simplified. On the other hand MU-MIMO requires full channel state information at the transmitter. It can be obtained by means of feedback in an FDD system or by exploiting channel reciprocity in a TDD system.

The results further show that the sum rate capacity in the measured channels is worse than the one in the uncorrelated synthetic channel. However, even in the measured channels DPC increases the sum rate capacity by a factor of 3.2 compared to SU-MIMO at high SNR using four transmit and four users with one receive antenna each. Linear precoding still increases the sum rate capacity by a factor of 2.7 at high SNR but provides little gains at low SNR.

7 Acknowledgements

Thanks to all the people at Eurecom helping with the measurement campaign.

References

- [1] D. Gesbert, M. Kountouris, R. W. Heath, C. B. Chae, and T. Salzer, "From single user to multiuser communications: Shifting the MIMO paradigm," *IEEE Signal Processing Magazine*, vol. 24, no. 5, pp. 36–46, Sept. 2007.
- [2] G. Caire and S. Shamai, "On the achievable throughput of a multiantenna gaussian broadcast channel," *IEEE Transactions on Information Theory*, vol. 49, no. 7, pp. 1691–1706, July 2003.
- [3] C. B. Peel, B. M. Hochwald, and A. L. Swindlehurst, "A vector-perturbation technique for near-capacity multiantenna multiuser communication-part I: channel inversion and regularization," *IEEE Transactions on Communications*, vol. 53, no. 1, pp. 195–202, Jan. 2005.

- [4] N. Jindal and A. Goldsmith, “Dirty-paper coding versus TDMA for MIMO broadcast channels,” *IEEE Transactions on Information Theory*, vol. 51, no. 5, pp. 1783–1794, May 2005.
- [5] R. de Lacerda, L. S. Cardoso, R. Knopp, M. Debbah, and D. Gesbert, “EMOS platform: real-time capacity estimation of MIMO channels in the UMTS-TDD band,” in *Proc. International Symposium on Wireless Communication Systems (IWCS)*, Trondheim, Norway, Oct. 2007.
- [6] G. Bauch, J.B. Anderson, C. Guthy, M. Herdin, J. Nielsen, J. A. Nossek, P. Tejera, and W. Utschick, “Multiuser MIMO channel measurements and performance in a large office environment,” in *Proc. IEEE Wireless Comm. and Net. Conf.*, Hong Kong, March 2007, pp. 1900–1905.
- [7] G. Bauch, P. Tejera, C. Guthy, W. Utschick, J. A. Nossek, M. Herdin, J. Nielsen, J. B. Andersen, E. Steinbach, and S. Khan, “Multiuser MIMO: Principle, performance in measured channels and applicable service,” in *Proc. IEEE Veh. Technol. Conf. (VTC)*, Dublin, Ireland, Apr. 2007, pp. 2053–2057.
- [8] G. W. K. Colman and T. J. Willink, “Limited feedback precoding in realistic MIMO channel conditions limited feedback precoding in realistic MIMO channel conditions,” in *Proc. IEEE Int. Conf. on Comm. (ICC)*, Glasgow, Scotland, June 2007, pp. 4363–4368.
- [9] M. Sharif and B. Hassibi, “A comparison of time-sharing, DPC, and beamforming for MIMO broadcast channels with many users,” *IEEE Transactions on Communications*, vol. 55, no. 1, pp. 11–15, Jan. 2007.
- [10] Lai-U Choi and R. D. Murch, “A transmit preprocessing technique for multiuser mimo systems using a decomposition approach,” *IEEE Transactions on Wireless Communications*, vol. 3, no. 1, pp. 20–24, Jan. 2004.
- [11] F. Boccardi, F. Tosato, and G. Caire, “Precoding Schemes for the MIMO-GBC,” in *Proc. of Int. Zurich Sem. on Comm. (IZS’06)*, Zurich, Switzerland, Feb. 2006.
- [12] Q. H. Spencer, A. L. Swindlehurst, and M. Haardt, “Zero-forcing methods for downlink spatial multiplexing in multiuser MIMO channels,” *IEEE Transactions on Signal Processing*, vol. 52, no. 2, pp. 461–471, Feb. 2004.
- [13] S. Vishwanath, N. Jindal, and A. Goldsmith, “Duality, achievable rates, and sum-rate capacity of gaussian MIMO broadcast channels,” *IEEE Transactions on Information Theory*, vol. 49, no. 10, pp. 2658–2668, Oct. 2003.
- [14] Wei Yu and J. M. Cioffi, “Sum capacity of gaussian vector broadcast channels,” *IEEE Transactions on Information Theory*, vol. 50, no. 9, pp. 1875–1892, Sept. 2004.
- [15] P. Viswanath and D. Tse, “Sum capacity of the vector gaussian broadcast channel and uplink-downlink duality,” *IEEE Transactions on Information Theory*, vol. 49, no. 8, pp. 1912–1921, Aug. 2003.
- [16] N. Jindal, Wonjong Rhee, S. Vishwanath, S. Jafar, and A. Goldsmith, “Sum power iterative water-filling for multi-antenna gaussian broadcast channels,” *IEEE Transactions on Information Theory*, vol. 51, no. 4, pp. 1570–1580, Apr. 2005.
- [17] E. Telatar, “Capacity of multi-antenna gaussian channels,” *European Transactions on Telecommunications*, vol. 10, pp. 585–595, 1999.

- [18] F. Kaltenberger, L. S. Cardoso, M. Kountouris, R. Knopp, and D. Gesbert, “Capacity of linear multi-user MIMO precoding schemes with measured channel data,” in *Proc. IEEE Intl. Workshop on Signal Processing Advances in Wireless Communications (SPAWC)*, Recife, Brazil, July 2008, submitted.